Hybrid Materials

Enhanced Catalytic Activity for Methanol Electro-oxidation of Uniformly Dispersed Nickel Oxide Nanoparticles—Carbon Nanotube Hybrid Materials

Xili Tong, Yong Qin, Xiangyun Guo,* Oussama Moutanabbir, Xianyu Ao, Eckhard Pippel, Lianbing Zhang, and Mato Knez**

Hybrid materials consisting of carbon nanotubes (CNTs) as support for metal oxide nanoparticles, often show extraordinary properties and are considered highly promising for numerous future applications such as electrochemical power sources,[1a,1b] photocatalysis,[1c] flexible piezoelectric generators,[1d] field-emission displays,[1e] and sensors.[1f] Two general strategies are commonly being applied for synthesizing such hybrid nanostructures: grafting bi-functional organic linkers to pre-synthesized nanoparticles and subsequently linking those nanoparticles to CNTs[2] or growing nanoparticles directly on CNTs by means of colloid chemistry.[3] In both cases, the strategies rely on initial modification of pristine CNTs. Even after modification, it is challenging to obtain highly dispersed nanoparticles with a uniform size distribution and without introduction of impurities on CNTs. However, both the size and the dispersion of metal oxide nanoparticles on the walls of CNTs, play a crucial role for the performance of such 1D hybrid nanostructures if catalysis is pursued. Simple and effective approaches for the controllable synthesis of such hybrid nanostructures, alternative to the above-mentioned, are desired for an optimized performance of the nanomaterials and are essential for future applications.

Dr. X. Tong, Prof. Y. Qin, Prof. X. Y. Guo
State Key Laboratory of Coal Conversion
Institute of Coal Chemistry
Chinese Academy of Sciences
Taiyuan 030001, China
E-mail: qinyong@sxicc.ac.cn; xyguo@sxicc.ac.cn
Dr. X. Tong, Dr. X. Ao, Dr. E. Pippel
Max Planck Institute of Microstructure Physics
Weinberg 2, 06120 Halle, Germany
Prof. O. Moutanabbir
Department of Engineering Physics
Ecole Polytechnique de Montreal
C. P. 6079, Succ. Centre-Ville, Montreal, QC, H3C 3A7, Canada
Dr. L. Zhang, Prof. M. Knez
CIC nanoGUNE Consolider, Tolosa Hiribidea 76
20018 Donostia-San Sebastian, Spain, Ikerbasque,
Basque Foundation for Science
Alameda Urquijo 36-5, 48011 Bilbao, Spain
E-mail: m.knez@nanogune.eu

DOI: 10.1002/smll.201200839

Atomic layer deposition (ALD) is a deposition method which allows growth of dense thin films with atomic-level precision in a layer-by-layer manner, but in certain circumstances also results in the growth of discrete nanoparticles.[4] The method is very sensitive to the surface chemistry of the substrate[5] and the deposition temperature.[6] Properly controlled, those parameters will turn ALD into a promising route for a controllable synthesis of nanoparticle/CNT hybrid structures with high precision. Eventually, catalysts with high performance may be obtained.

In recent years, several methods have been reported for the fabrication of NiO/CNT hybrid material for use as advanced electrocatalysts due to its unique hybrid structure, large surface area, and high electrochemical activity.[7] However, it is still difficult to permit precise control of the size of the deposited NiO nanoparticles at the sub-nanometer level while preserving the homogeneity; thus there have been no reports of the controllable construction of NiO nanoparticles supported on pristine CNTs by ALD. It is commonly accepted that, due to the lack of dangling bonds, it is difficult to directly deposit metal oxides on pristine CNTs, in particular at low temperatures.[8] An advance modification of CNTs is the method of choice for the successful growth of nanoparticles atop.[9] For example, Sun et al. reported that the deposition of ultra-fine SnO_2 nanoparticles by ALD can only be performed if the carbon nanotubes are highly nitrogen-doped.[8a] Park et al. found that, due to the chemical inertness of CNTs, a ZnO-ALD process will lead to nanoparticles growing on defect sites and/or impurities of single-walled CNTs only.[8b] Hwang et al. showed that by ALD, ZnO nanoparticles could be deposited on a forest of single-walled CNTs if those show a small amount of oxygen- or hydroxyl-containing defects and/or impurities on their walls.[8c] In this work, we apply ozone as one ALD precursor. Compared to water, which is frequently used as an oxygen source in ALD processes, O_3 is a strong oxidizing agent, which effectively provides functionalization of pristine CNTs. In this way, an advance modification of CNTs is avoided, and the functionalization of the CNTs occurs simultaneously as the nanoparticle deposition. O_3 acts both as agent for defect site formation as well as counter-precursor for the ALD process; hence the formation of the hybrid material becomes more simplified. Alternated with a nickel precursor, a controllable deposition of discrete NiO

NANO MICRO small

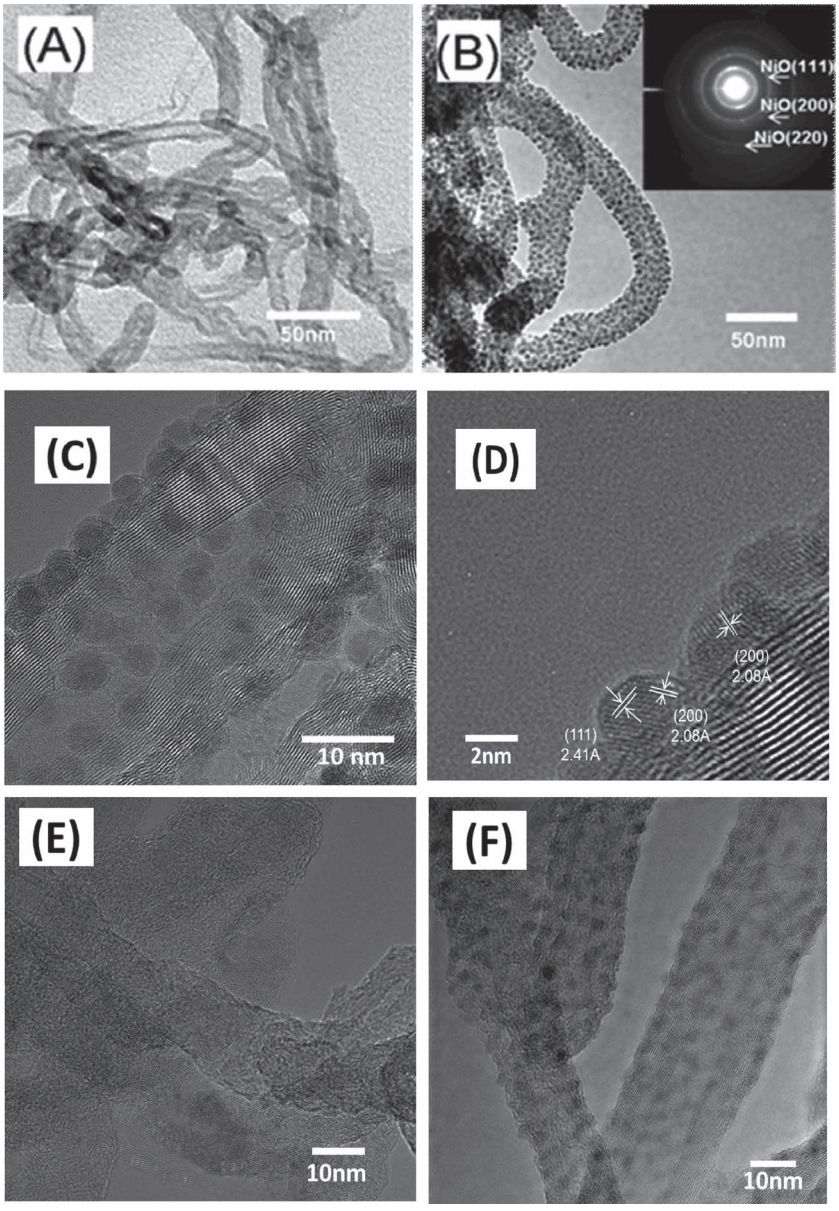

Figure 1. TEM images of A) pristine CNTs and B) NiO nanoparticles on CNTs grown after 400 ALD cycles (inset shows the SAED pattern). C) HRTEM image of a NiO/CNT hybrid nanostructure after 400 ALD cyclesand of D) the area boxed region in (C) at higher magnification showing the {200} and {111} planes of cubic NiO. HRTEM image at lower magnification of E) pristine CNTs and F) a NiO/CNT hybrid nanostructure after 400 ALD cycles.

nanoparticles on pristine CNTs at moderate temperatures is realized. The NiO nanoparticles are highly dispersed on the walls of CNTs, and their sizes are controlled by the ALD process parameters. The obtained unique NiO/CNT hybrid structures exhibit outstanding performance in catalysis, which is demonstrated by the electro-oxidation of methanol.

Pristine multi-walled CNTs (MWCNTs, purchased from Sigma Aldrich) with diameters in the range of 12–26 nm (**Figure 1**A) were used as the substrate for the growth of NiO nanoparticles. The ALD process was performed with bis(cyclopentadienyl) nickel (Cp_2Ni) and O_3 as the Ni precursor and oxygen source, respectively. The deposition was conducted with a substrate temperature of 140 °C. Figure 1B shows a typical transmission electron microscopy (TEM) image of the obtained NiO nanoparticle/CNT hybrid nanostructures, exhibiting a uniform dispersion of discrete NiO nanoparticles on the CNTs. The diffraction rings in the selected area electron diffraction (SAED) pattern (inset in Figure 1B) of the nanoparticles can be indexed to the cubic phase NiO (Joint Committee on Powder Diffraction Standards (JCPDS) 4-0835). High-resolution TEM (HRTEM) investigations were conducted in order to investigate the crystalline structure of the NiO nanoparticles. Figure 1C reveals that the discrete NiO nanoparticles have an average particle size of 4.9 nm. The interplanar spacing of 2.08 and 2.41 Å (Figure 1D) matches well with the (200) and (111) plane of cubic NiO, demonstrating that the supported nanoparticles are indeed NiO nanocrystals. Furthermore, varying the number of ALD cycles can be used to very comfortably control the size of the NiO nanoparticles. For example, the average NiO particle diameters measured by TEM are 1.5, 3.3, 4.9, and 6.3 nm after 100, 200, 400, and 600 cycles, respectively (Figure S1, Supporting Informaiton (SI)). The standard deviation of the size of NiO nanoparticles is 0.1, 0.1, 0.2, and 0.2 nm for 100, 200, 400, and 600 ALD cycles, respectively, indicating that high uniformity in the particle size can be maintained during the nucleation and growth of the nanoparticles (Figure S2, SI). In order to observe the dispersion and uniformity of NiO nanoparticles supported on CNTs, HRTEM images of pristine CNTs at low magnification (Figure 1E) and NiO/CNTs hybrid structure (Figure 1F) were obtained. It can be seen that NiO nanoparticles having a uniform size distribution and high-quality dispersion throughout the entire surface of the CNTs can be achieved.

A plausible reaction mechanism for the ALD of NiO on CNTs is schematically illustrated in **Figure 2**. It was demonstrated that MWCNTs exhibit a large number of carbonaceous debris on their surface, which is difficult to be characterized, but significantly interferes with the functionalization.[10] In the first step, O_3 will preferentially oxidize these carbonaceous debris on the outer wall of the CNTs.[11] This oxidation effect may be enhanced from the fact that the π-electron density at the concave interior surface and the convex exterior wall of the CNTs is different due to the curved tubular structure.[12] The shift in electron density favors the attack of the strongly oxidizing agent and permits the creation of defect sites. In the Fourier transform infrared (FTIR) spectrum of pristine CNTs (Figure S3, SI),

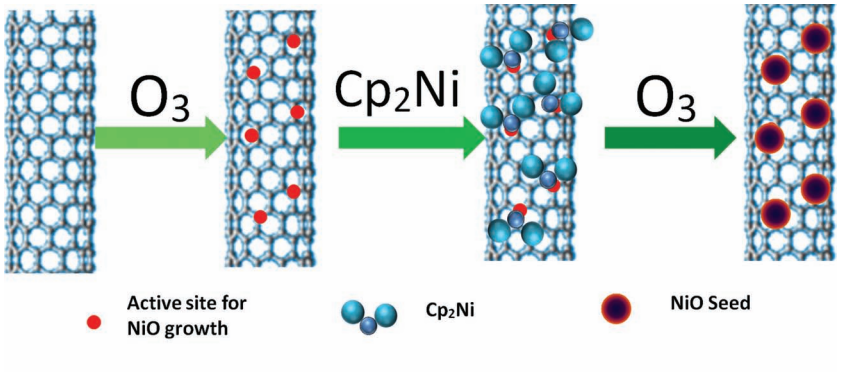

Figure 2. Schematic illustration of the proposed ALD growth initiation of NiO nanoparticles on a CNT.

three obvious peaks appearing between 2850 and 3000 cm^{-1} can be assigned to the C−H stretching in pristine CNTs.[13] These disappear after the O_3 treatment. On the other hand, the peak at around 3300 cm^{-1}, characteristic for O–H stretching, becomes more pronounced after the O_3 treatment, indicative of more oxygen being available on the walls of the ALD-treated CNTs. Raman analysis (Figure S4, SI) of all investigated CNTs display two bands centered around 1360 (D band) and 1585 cm^{-1} (G band), which is characteristic for CNTs.[14] The small shoulder at ~1620 cm^{-1} is attributed to the D′ band. It is noticeable that the absolute intensity of D and G bands increases with the number of ALD cycles indicating that more defects and more roughness are produced in the CNT samples during the process. After 500 cycles, a strong attenuation of the Raman signal is observed. A close examination of the Raman data shows that the ALD treatment induces subtle but important changes in the Raman modes of the CNTs. In particular, post-ALD modes were found to shift by 2–3 cm^{-1} to higher wavenumbers. A similar shift was observed earlier by Osswald et,al., which was ascribed to the oxidation of CNTs.[15] This shift is associated with a narrowing of Raman modes and can be clearly observed in the Raman spectra normalized with the G band (Figure S5, SI). Note that the D′ band is expressed more strongly after ALD processing, which is due to the sharpening of the G band simultaneously to an increase of the D-to-G-band-intensity ratio (Figure S5, SI), thereby providing additional evidence of oxidation and defect formation. These highly dispersive defects and oxygen-containing active sites are likely to become anchoring sites for the Ni precursor chemisorption. Upon adsorption, initially the two cyclopentadienyl groups of the Cp_2Ni molecule will guide the dispersion of the adsorbed molecules, due to steric effects. Subsequently, O_3 will react with the Ni precursor to form highly dispersed NiO seeds at moderate temperatures. Because the density of surface anchoring sites is not high enough to allow the ALD precursors to react uinformly with the substrate, an island growth mode is favored.[16] In this case, deposition occurs preferentially onto the NiO seeds already deposited in preceding cycles, which will continue to grow to NiO nanoparticles with an advancing number of ALD cycles.

The change of the surface state of the NiO/CNT hybrid structure can be observed by mapping intermediate states of the nanostructures with energy-dispersive X-Ray spectroscopy (EDX). **Figure 3**A shows a typical scanning TEM (STEM) high-angle annular dark-field image of the NiO/CNT hybrid structure, where the bright features show NiO. Figure 3B–D show EDX maps of carbon, nickel, and oxygen, respectively. Figure 3 is indicative of the formation of numerous defects and oxidized sites on the wall of the pristine CNTs during the O_3 treatment. The active sites are uniformly distributed on the walls of pristine CNTs due to the extreme integrity and smoothness of the surface of pristine CNTs. Those defects act as nucleation sites for the formation of NiO nanoparticles in a well-dispersed manner

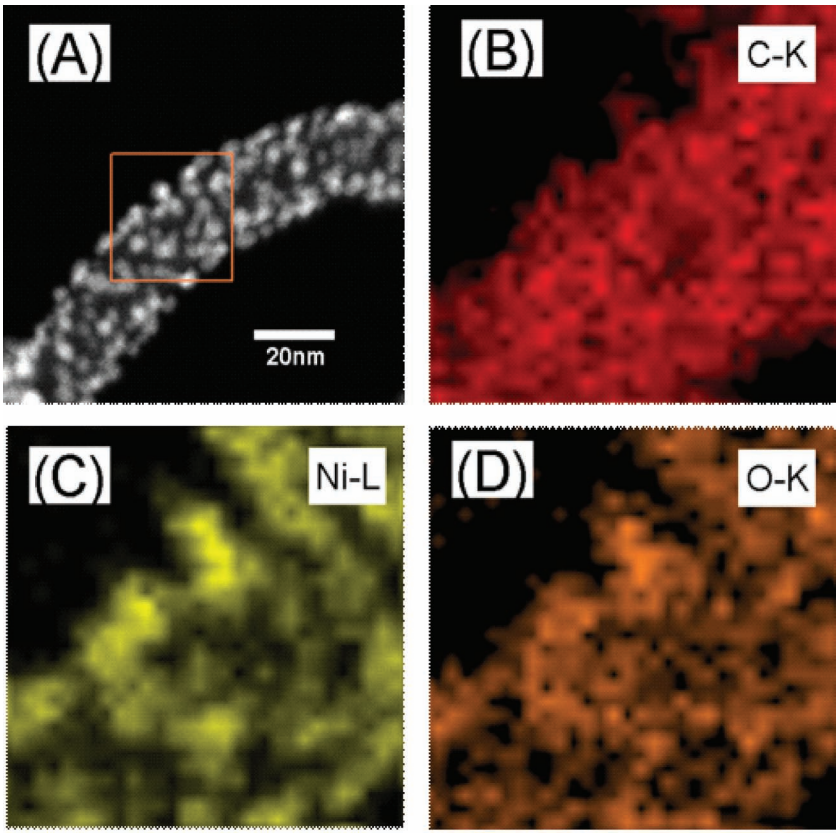

Figure 3. Element analysis of a NiO/CNT nanostructure. A) High-angle annular dark-field STEM image. B–D) Elemental maps of the boxed area in (A) for carbon (B), nickel (C), and oxygen (D).

NANO MICRO small

as shown in Figure 3C and D. Hence, the NiO nanoparticles resulting from the next processing step are also highly dispersed. The element composition of a catalyst is an important issue for its performance. In this work, we want to characterize the NiO/CNT hybrid, and therefore the composition of the metal oxide is of great relevance. The element content of Ni and O was measured to be 79.3 and 20.7 wt% by point analysis on the CNT wall, respectively (Figure S6, SI). This result is different from Bachmann's observation,[17] where the obtained nickel oxide film without the CNT support is nickel-deficient consisting of 76 wt% Ni and 24 wt% O. The reason for the difference can possibly be attributed to the temperature applied for the ALD process, which in our case is lower than that in Bachmann's work. The reactivity of O_3 at the temperatures applied in this work is relatively low, which leads to fewer defects in NiO nanocrystals.

NiO nanomaterials are important subjects of investigation in the fields of microelectronics,[18] electrochemical powering,[19] and biosensorics.[20] One very important characteristic of NiO is its activity as a catalyst for the oxidation of alcohols in fuel cells.[21] The mechanism of the electro-oxidation of methanol over NiO is shown below:[22]

$$NiO + OH^- \rightarrow NiOOH + e^- \quad (1)$$

$$NiOOH + CH_3OH \rightarrow Ni(OH)_2 + \text{Product} \quad (2)$$

$$Ni(OH)_2 + OH^- \rightarrow NiOOH + H_2O + e^- \quad (3)$$

Pure NiO possess inferior electrochemical activity because of its poor electrical conductivity; therefore supporting substrates with high conductivity, stable physical and chemical properties, and high specific surface area are needed to enhance the eletrocatalytic performance of NiO nanomaterials. From thermogravimetric–differential thermal analysis (TG-DTA) analysis (Figure S7, SI), the loading of NiO nanoparticles on CNTs is 6, 13, 26, and 40 wt% for NiO after 100, 200, 400, and 600 cycles, respectively. **Figure 4**A displays cyclic voltammograms (CV) of different NiO/CNT samples measured at a scan rate of 50 mV/s. The sharp anodic peak at 0.35 V is related to the oxidation of NiO to NiOOH, and the sharp cathodic peak at about 0.28 V is due to the reverse process. The insert of Figure 4A shows a pair of broad anodic and cathodic peaks for commercial NiO nanopowder. It is obvious that in direct comparison, the electrochemical activity of the NiO nanomaterials is better, which can be directly associated with the supporting CNTs. The oxidation peak current versus the mass of loaded NiO, as a function of the particle size, is shown in Figure 4B. The electrochemical activity of NiO/CNT hybrids increases with the NiO particle size until it reaches a maximum at around 4.9 nm. The electrochemical activity of NiO nanoparticles increases gradually by 2.3 times with the particle size growing from 1.5 to 4.9 nm and then decreases sharply when the particle size exceeds 4.9 nm. The very evident nanosize-effect of the NiO nanoparticles may be related to the differing number of defects on the crystalline face and the dispersion of the NiO nanoparticles in their varying sizes.[23] The electrochemical activity of the 4.9 nm NiO/CNT sample is about 88 times higher than that of commercial NiO nanopowder (<50 nm), about 23 times higher than the NiO/CNTs reported by Lin et al.,[24] and 10 times higher than the NiO/CNTs reported by Nam et al.[23b] We attribute this outstanding performance to the higher dispersion and uniformity of the NiO nanoparticles of the NiO/CNTs samples in our case.

In order to evaluate the electro-catalytic activity of NiO/CNT hybrid structures in terms of electro-oxidation of methanol, CVs were collected in a N_2-saturated solution of 1 M KOH containing 0.5 M CH_3OH at a scan rate of 50 mV/s. Figure 4C shows typical CVs of a NiO/CNT hybrid with a glassy carbon electrode, modified with 400 ALD cycles, in the absence and presence of methanol. The plot shows that the electro-oxidation of methanol over NiO/CNT hybrid nanostructures occurs with a high current value near 0.45 V. The 1D NiO/CNT hybrid structures can easily form a porous network, which can effectively facilitate the ion transport into the modified electrode and significantly increase the reactive surface area. As a result, the NiO/CNT hybrid nanostructures exhibit high performance in the electro-catalytic oxidation

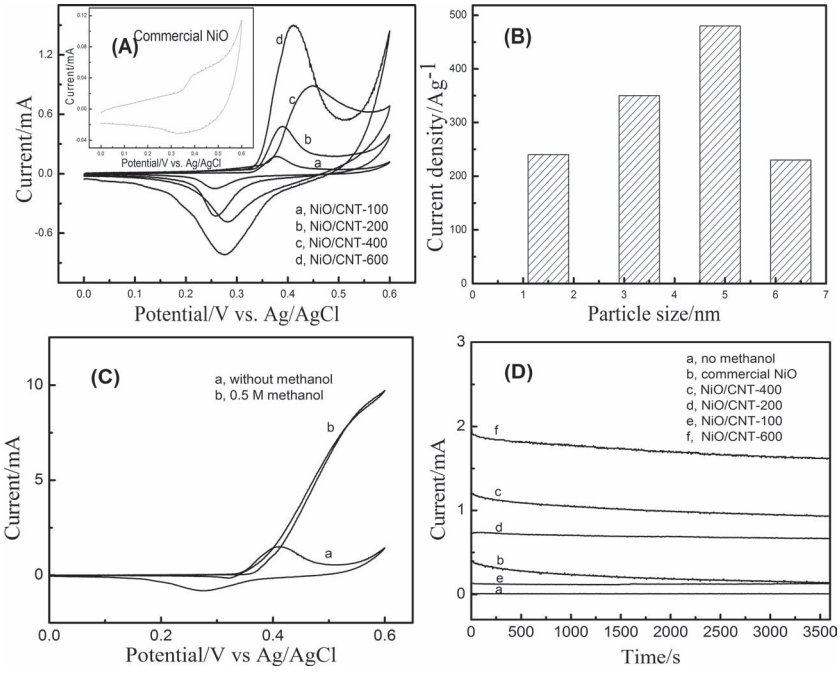

Figure 4. A) Cyclic voltammograms of different NiO/CNT samples in 1 M KOH solution at a scan rate of 50 mV/s.B) The oxidation peak current density as a function of the NiO particle size. C) Typical cyclic voltammograms of a NiO/CNT-400 sample (where the number refers to the number of ALD cycles) in 0.5 M methanol +1 M KOH solution at a scan rate of 50 mV/s. D)Chrono-amperometry of various NiO samples in 0.5 M methanol +1 M KOH solution at the potential of 0.45 V.

of methanol. The CVs of further NiO/CNT hybrid-modified glassy carbon electrodes in the presence of methanol are shown in Figure S8, SI. Chrono-amperometry profiles of both the NiO/CNT hybrid structures and commercial NiO nanopowder at 0.45 V were recorded in a N_2-saturated solution of 1 M KOH containing 0.5 M CH_3OH for a duration of 3600 s. Figure 4D shows that the stable-state current decay rate of the NiO/CNT catalysts is at least 4 times slower than that of the commercial NiO nanopowder, indicating that the NiO/CNT hybrid structure possesses good tolerance against reaction intermediates and may be applicable for long-term application as anode material in fuel cells. The enhanced stability results from the stronger interactions between the NiO nanoparticles and CNTs due to the presence of chemical bonds, which prevent the NiO nanoparticles from dissolution, Ostwald ripening, and aggregation.[25]

In conclusion, we have developed a simple and effective route for the synthesis of NiO nanoparticles with good crystallinity and uniform dispersion on pristine CNTs by ALD. Ozone is used as one of the two precursors and acts both as oxidizing agent for the CNTs and as oxygen source for the NiO growth. The sizes of the NiO nanoparticles range from 1.5 to 6.3 nm and can be precisely controlled by varying the number of ALD cycles. In the given size range, the size-dependency and mass electrochemical activity of the redox reaction of NiO in KOH solution is determined. Compared to commercial NiO nanopowder and the results reported by Asgari et al.,[7d] the obtained NiO/CNT hybrid nanostructures show greatly enhanced electrochemical catalytic ability and stability for a methanol oxidation reaction. Our synthesis route is not specific for NiO and can be adapted to produce further metal oxide/CNT hybrid nanostructures, promising a large bandwidth of materials for catalytic methanol oxidation or other advanced catalytic reactions.

Experimental Section

ALD was carried out in a home-made hot-wall closed chamber-type ALD reactor (Halle, Germany) equipped with a quartz crystal microbalance that combines a low-vacuum system based on a rotary vane pump, utilizing N_2 as a precursor carrier and purge gas at a pressure of 2 Torr. The O_3 was produced using an O_3 generator (Ozone Engineering L11), and the temperature of the bis(cyclopentadienyl)nickel(II) precursor was maintained at 80 °C. The deposition was conducted with a substrate temperature of 140 °C. In the first step, MWCNTs were dispersed into absolute ethanol under sonication for 5 min. Subsequently, suspensions of carbon nanotubes were dispersed by spin-coating and dried on a Si wafer. The sample was transferred to the ALD chamber for the NiO nanoparticle growth. The pulse, exposure, and purge times for the bis(cyclopentadienyl)nickel(II) precursor were 1, 2, and 2 s, respectively, and for the O_3, 1, 10, and 5 s, respectively.

The electrochemical experiments were controlled with a 263A potentiostat/galvanostat (Princeton Applied Research). The NiO/CNT glassy carbon (NiO/CNT–GC. Caution: NiO nanoparticles are highly toxic,[26] please obtain special instruction before use. Wear protective gloves if exposed or concerned) electrode was prepared as follows. A glassy carbon (GC) electrode (3 mm in diameter, 7 mm^2) was carefully polished with 0.3 μm and subsequently with 0.05 μm alumina on polishing cloth, then ultrasonicated in 0.1 M HNO_3 for 3 min, and finally washed with acetone. NiO samples (1 mg), 5 wt.% Nafion solution (10 μL), and ethanol (1.0 mL) were mixed by ultrasonication. The as-prepared mixture (10 μL) was then transferred onto the polished GC electrode with a syringe, and dried in air. A Pt wire electrode and a Ag/AgCl electrode (A. J. Cope & Son Ltd, double-junction, saturated KCl) were utilized as the counter electrode and the reference, respectively.

Supporting Information

Supporting Information is available from the Wiley Online Library or from the author.

Acknowledgements

X.T., Y.Q., and X.Y.G. greatly acknowledge financial support from the in-house project of SKLCC (Y1BWLI1991 and Y0BWLC1991). X.T., L.Z., and M.K. greatly acknowledge financial support from the German Ministry of Research and Education (BMBF, FKZ 03 × 5507).

[1] a) J. Ye, H. F. Cui, X. Liu, T. M. Lim, W. Zhang, F. Sheu, *Small* **2005**, *1*, 560; b) J. Kim, K. H. Lee, L. J. Overzet, G. S. Lee, *Nano Lett.* **2011**, *11*, 2611; c) Y. Zhang, Z. Tang, X. Fu, Y. Xu, *ACS Nano* **2010**, *4*, 7303; d) C. J. Hu, Y. H. Lin, C. W. Tang, M. Y. Tsai, W. K. Hsu, H. F. Kuo, *Adv. Mater.* **2011**, *23*, 2941; e) C. J. Yang, J. I. Park, Y. R. Cho, *Adv. Eng. Mater.* **2007**, *9*, 88; f) M. Willinger, G. Neri, E. Rauwel, A. Bonavita, G. Micali, N. Pinna, *Nano. Lett.* **2008**, *8*, 4201.

[2] a) L. Sheeney-Haj-Khia, B. Basnar, I. Willner, *Angew. Chem.* **2005**, *117*, 78; *Angew. Chem. Int. Ed.* **2005**, *44*, 78; b) M. Olek, T. Busgen, M. Hilgendorff, M. Giersig, *J. Phys. Chem. B* **2006**, *110*, 12901.

[3] a) B. H. Juarez, C. Klinke, A. Kornowski, H. Weller, *Nano Lett.* **2007**, *7*, 3564; b) M. Sathiya, A. S. Prakash, K. Ramesha, J-M. Tarascon, A. K. Shukla, *J. Am. Chem. Soc.* **2011**, *133*, 16291; c) B. Yoon, C. M. Wai, *J. Am. Chem. Soc.* **2011**, *127*, 17174.

[4] a) S. M. George, *Chem. Rev.* **2010**, *110*, 111; b) Y. Qin, L. Liu, R. Yang, U. Gösele M. Knez, *Nano Lett.* **2008**, *8*, 3221; c) M. Knez, K. Nielsch, L. Niinistö, *Adv. Mater.* **2007**, *19*, 3425; d) T. J. Knisley, T. C. Ariyasena, T. Sajavaara, M. J. Saly, C. H. Winter, *Chem. Mater.* **2011**, *23*, 4417.

[5] E. Färm, S. Lindroos, M. Ritala, M. Leskelä, *Chem. Mater.* **2012**, *24*, 275.

[6] X. Meng, Y. Zhong, Y. Sun, M. N. Banis, R. Li, X. Sun, *Carbon* **2011**, *49*, 1133

[7] a) W. Zhang, J. Chen, L. Jiang, Y. Yu, J. Zhang, *Microchim Acta* **2010**, *168*, 259; b) C. Xu, J. Sun, L. Gao, *J. Power Sources* **2011**, *196*, 5138; c) J. Y. Lee, K. Liang, K. H. An, Y. H. Lee, *Synth. Met.* **2005**, *150*, 153; d) M. Asgari, M. G. Maragheh, R. Davarkhah, E. Lohrasbi, *J. Electrochem. Soc.* **2011**, *158*, K225; e) R. P. Deo, N. S. Lawrence, J. Wang, *Analyst* **2004**, *128*, 1076.

[8] a) X. Wang, S. M. Tabakman, H. Dai, *J. Am. Chem. Soc.* **2008**, *130*, 8152; b) Y. Lu, S. Bangsaruntip, X. Wang, L. Zhang, Y. Nishi,

H. Dai, *J. Am. Chem. Soc.* **2006**, *128*, 3518; c) D. B. Farmer, R. G. Gordon, *Nano Lett.* **2006**, *6*, 699.
[9] a) Y. Chen, J. Wang, X. Meng, Y. Zhong, R. Li, X. Sun, S. Ye, S. Knights, *Int. J. Hydrogen Energy* **2011**, *36*, 11085; b) Y. Min, E. J. Bae, J. B. Park, U. J. Kim, W. Park, J. Song, C. S. Hwang, N. Park, *Appl. Phys. Lett.* **2007**, *90*, 263104; c) Y. Min, H. Lee, Y. H. Lee, C. S. Hwang, *Cryst. Eng. Comm.* **2011**, *13*, 3451.
[10] C. G. Salzmann, S. A. Llewellyn, G. Tobias, M. A. H. Ward, Y. Huh, M. L. H. Green, *Adv. Mater.* **2007**, *19*, 883.
[11] D. B. Mawhinney, V. Naumenko, A. Kuznetsova, J. T. Yates, *J. Am. Chem. Soc.* **2000**, *122*, 2383.
[12] a) R. C. Haddon, *Science* **1993**, *261*, 1545–1550; b) D. Ugarte, A. Chatelain, W. A. de Heer, *Science* **1996**, *274*, 1897.
[13] H. Luo, Z. Shi, N. Li, Z. Gu, Q. Zhuang, *Anal. Chem.* **2001**, *73*, 915.
[14] D. H. Lee, J. A. Lee, W. J. Lee, D. S. Choi, W. J. Lee, S. O. Kim, *J. Phys. Chem. C* **2010**, *114*, 21184.
[15] S. Osswald, M. Havel, Y. Gogotsi, *J. Raman Spectrosc.* **2007**, *38*, 728.
[16] C. Marichy, J. Tessonnier, M. C. Ferro, K. Lee, R. Schlögl, N. Pinna, M. Willinger, *J. Mater. Chem.* **2012**, *22*, 7323.
[17] J. Bachmann, A. Zolotaryov, O. Albrecht, S. Goetze, A. Berger, D. Hesse, D. Novikov, K. Nielsch, *Chem. Vap. Deposition* **2011**, *17*, 177.
[18] a) A. P. LaGrow, B. Ingham, S. Cheong, G. V. M. Williams, C. Dotzler, M. F. Toney, J. D. A. Efferson, E. C. Corbos, P. T. Bishop, J. Cookson, R. D. Tilley, *J. Am. Soc. Chem.* **2012**, *134*, 855; b) L. He, Z. Liao, H. Wu, X. Tian, D. Xu, G. L. W. Cross, G. S. Duesberg, I. V. Shvets, D. Yu, *Nano. Lett.* **2012**, *11*, 4601.
[19] Q. Lu, M. W. Lattanzi, Y. Chen, X. Kou, W. Li, X. Fan, K. M. Unruh, J. G. Chen, J. Q. Xiao, *Angew. Chem.* **2011**, *123*, 6979; *Angew. Chem. Int. Ed.* **2011**, *50*, 6847.
[20] a) S. Mohan, P. Srivastava, S. N. Maheshwari, S. Sundar, R. Prakash, *Analyst* **2011**, *136*, 2845; b) M. Shamsipur, M. Najafi, M. M. Hosseini, *Bioelectrochemistry* **2010**, *77*, 120.
[21] a) N. Spinner, W. E. Mustain, *Electrochim. Acta* **2011**, *56*, 5656; b) I. Danaeea, M. Jafariana, F. Forouzandeha, F. Gobal, M. G. Mahjani, *Int. J. Hydrogen Energy* **2008**, *33*, 4367.
[22] M. A. Abdel Rahim, R. M. Abdel Hameed, M. W. Khalil, *J. Power Sources* **2004**, *134*, 160.
[23] a) M. Shao, A. Peles, K. Shoemaker, *Nano Lett.* **2011**, *11*, 3714; b) S. H. Nam, Y. Kim, H. Shim, S. M. Choi, H. J. Kim, W. B. Kim, *J. Nanosci. Nanotechnol.* **2008**, *8*, 5427.
[24] P. Lin, Q. She, B. Hong, X. Liu, Y. Shi, Z. Shi, M. Zheng, Q. Dong, *J. Electrochem. Soc.* **2010**, *157*, A818.
[25] a) S. Guo, S. Zhang, X. Sun, S. Sun, *J. Am. Chem. Soc.* **2011**, *133*, 15354. b) R. L. Puurunen, *J. Appl. Phys.* **2005**, *97*, 121301.
[26] M. Horie, K. Nishio, K. Fujita, H. Kato, A. Nakamura, S. Kinugasa, S. Endoh, A. Miyauchi, K. Yamamoto, H. Murayama, E. Niki, H. Iwahashi, Y. Yoshida, J.Nakanishi, *Chem. Res. Toxicol.* **2009**, *22*, 1415.

Received: April 19, 2012
Revised: June 11, 2012
Published online: August 2, 2012

